A Direct Matrix Approach to 3-D Antenna Radiation-Pattern Estimation from Partially-Scanned Spherical Near-Field Data

Taeyoung Yang and William A. Davis

Virginia Tech Antenna Group, 302 Whittemore (0111), Blacksburg, VA 24061-111, USA

{mindlink, wadavis}@vt.edu

Abstract

Far-field radiation-pattern estimation is explored for the case of partially-scanned spherical near-field data resulting from physical limitations of an antenna under test or associated measurement systems. A direct matrix approach, based on spherical-wave expansions, is found to be simple and effective for constructing the 3-D radiation pattern from partially-scanned near-field data. Criteria to determine the minimum near-field data for full 3-D pattern reconstruction is explained. The concept of the direct matrix approach is demonstrated for a mobile antenna and a horn antenna. An additional benefit of this approach is the reduction of the scan time for antenna measurements.

1. Introduction

The antenna radiation pattern is one of the most important antenna characterization factors. The radiation pattern can be directly measured in a far-field range. Alternatively, one can obtain the pattern through a near-field-to-far-field transformation of measured near-field data. Although near-field ranges typically require extra computation and accurate amplitude and phase measurements, near-field ranges are often preferred to a far-field range because they are compact and less prone to issues of multipath. Unfortunately, a full-angle scan cannot always be accomplished in a near-field range due to physical limitations of either the antenna under test (AUT) or the associated measurement system. Thus, it is of interest to investigate the possible determination of the entire 3-D far-field pattern of an antenna from the near-field scan over a subset of the desired angular space.

Because an exact-field distribution can only be modeled with an infinite number of expansion terms, truncation errors are always involved in modeling. Some researchers have been working on the mitigation of truncation errors in the near-field to far-field transform [1, 2]. However, the problem of obtaining an antenna radiation pattern from partially-scanned near-field data introduces an additional source of truncation error. Wittmann, *et al* [3], investigated pattern estimation from partially-scanned far-field data based on the spherical wave expansion (SWE) [4]. They used a least-squares solution approach and singular-value decomposition in order to filter the truncation errors. They presented some examples for 2-D pattern estimation.

In this paper, we consider the near-field to far-field transform for partially-scanned spherical near-field data. A direct matrix approach with a pseudo inverse is presented to estimate the full 3-D far-field pattern. Examples for omni-directional and directional antennas are considered to demonstrate the effectiveness of the direct matrix approach. To obtain a better understanding of the highest-order spherical mode number (N), the maximum directivity, and the distance between the AUT and probe needed for of the estimation, we explore spherical-mode excitation and the related antenna range issues in the next section.

2. Spherical Mode Excitation and Radiation Zone

Radiating fields in free space can be represented with the second-kind spherical Hankel function ($\hat{H}_n^{(2)}$) and the first-kind associated Legendre function (P_n^m) with an $exp(j\omega t)$ time dependence. For example, the transverse electric fields can be expressed at distance r_0 as the following [4]:

$$E_\theta(r_0,\theta,\phi) = -j\sum_{m,n}\left[f_{mn}\frac{m}{\sin\theta}P_n^{|m|}(\cos\theta)+a_{mn}\frac{d}{d\theta}P_n^{|m|}(\cos\theta)\right]e^{jm\phi} \tag{1}$$

$$E_\phi(r_0,\theta,\phi) = \sum_{m,n}\left[f_{mn}\frac{d}{d\theta}P_n^{|m|}(\cos\theta)+a_{mn}\frac{m}{\sin\theta}P_n^{|m|}(\cos\theta)\right]e^{jm\phi}, \tag{2}$$

where a_{mn} and f_{mn} are scaled versions of the magnetic (A_{mn}) and electric (F_{mn}) mode-coupling coefficients, i.e.,

$$a_{mn} = \eta_0\hat{H}_n^{(2)\prime}(kr_0)A_{mn}/r_0 \text{ and } f_{mn} = \hat{H}_n^{(2)}(kr_0)F_{mn}/r_0. \tag{3}$$

978-1-4244-6051-9/11/$26.00 ©2011 IEEE

Each combination of m and n indicates a spherical mode. The excited spherical modes and the corresponding coupling coefficients can be found through spherical-wave expansions (SWE) [4] by using the orthogonal properties of the associated Legendre functions. Once we have the decomposed spherical modes, we can characterize the electric and magnetic fields at any region (near or far) outside the antenna test sphere.

The normalized electric and magnetic-field strengths versus distance from the antenna are shown in Figure 1 for some spherical TM_{mn} modes at 1.5 GHz. The field strengths are shown relative to their asymptotical far-field variations to emphasize the apparent separation of the modes into radiation and near-field regions. Both electric and magnetic fields of each mode appear to be in the far-field region at approximately n/k, where k is the wave number ($2\pi/\lambda_0$). Therefore, one can estimate a criterion for far-field distance if the highest-order spherical mode number (N) is known. As illustrated in Figure 2, the far-field region criterion based on the concept of the spherical mode excitation would be $\lambda_0 N/(2\pi)$, compared to the conventional far-field region criterion, $max\{D, \lambda_0, 2D^2/\lambda_0\}$ [5], where D is the largest dimension of antenna. Notice that the reactive fields of all the excited spherical modes, including the fundamental mode, overlap in the radian sphere (ka = 1) where the reactive fields dominate the total fields. Thus, it is typically recommended that the probe not be located inside the reactive rear-field region for near-field scanning. Compensation of the potential interaction between the antenna under test and the probe is generally neglected. Generally, only the probe pattern effect is considered [4].

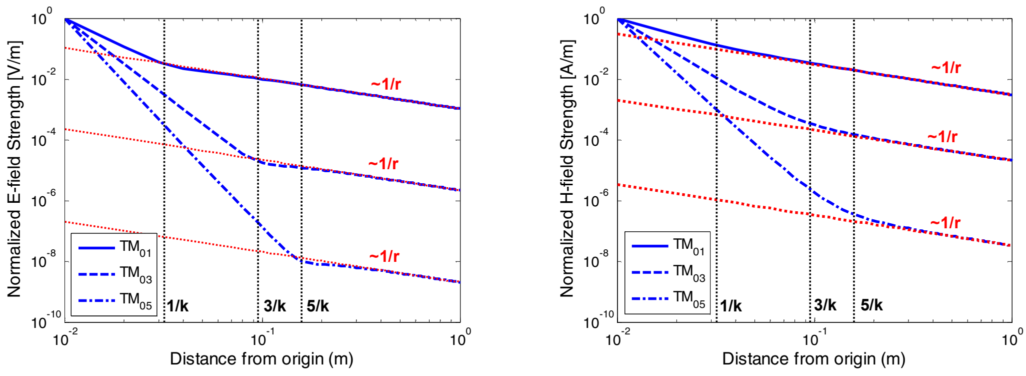

(a) (b)

Figure 1. Normalized field strength comparison for some spherical TM modes with their asymptotical far-field variations at 1.5 GHz – (a) Electrical fields and (b) Magnetic fields.

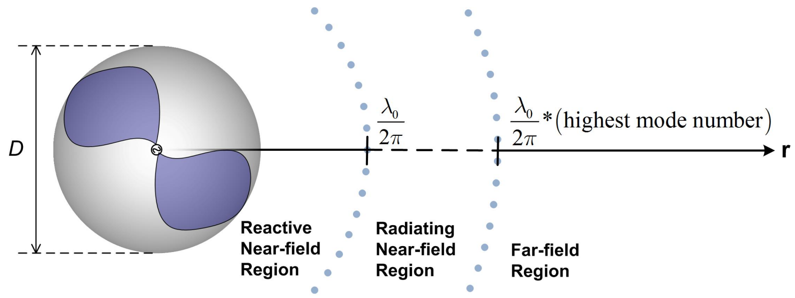

Figure 2. Antenna field regions and their criteria with respect to excited spherical modes.

The maximum radiation directivity of the antenna under test is also related the highest-order spherical mode number (N). In theory, the maximum directivity of an antenna is not limited by antenna size, but limited by the number of practically-excited spherical modes. Harrington [6] estimated the maximum radiation directivity of an antenna (D_{max}) in terms of the highest-order spherical mode number (N) for a lossless case, i.e. 100 % radiation efficiency (G_{max} = D_{max}) , and found

$$D_{max} = N^2 + 2N \,. \tag{4}$$

Alternatively, the maximum directivity can be estimated in terms of the maximum effective aperture (A) from [5]

$$D_{max} = 4\pi A / \lambda_0^2 \,. \tag{5}$$

Therefore, we may estimate the highest-order spherical mode number (N) by relating Eqs. (4) and (5). The far-field distance can then be estimated from this estimated N, as discussed above.

3. Pattern Estimation from Partially-Scanned Near-Field Data

In fact, spherical fields can be written in several ways [4], using integral, matrix [7], and Fourier transform (far fields) approaches, which essentially represent an infinite summation of the spherical modes. Alternatively, one can write the spherical fields in terms of equivalent sources exciting these spherical modes, similar to the method of moments (MoM) approach of Sarkar [8]. Sarkar's approach allows the selection of basis and weighting functions for the spherical fields and evaluation of the equivalent sources. A direct matrix approach is an alternative that may not be computationally efficient, but the matrix approach is simple and straight forward for obtaining the far-field estimation from partially-scanned spherical near-field data.

The matrix form for the two transverse components of the electric field can be written as follows to obtain the spherical coupling coefficients in Eqs. (1) and (2) with sampled data in θ and ϕ:

$$\begin{bmatrix}[f_{mn}]\\ [a_{mn}]\end{bmatrix} = \begin{bmatrix}\begin{bmatrix}\dfrac{m}{\sin\theta_p}P_n^{|m|}(\cos\theta_p)e^{jm\phi_q}\end{bmatrix} & \cdots \\ \vdots & \ddots\end{bmatrix}^{\dagger} \begin{bmatrix} j\left[E_\theta(\theta_i,\phi_k)\right] \\ \left[E_\phi(\theta_i,\phi_k)\right]\end{bmatrix} \triangleq [\mathbf{P}]^\dagger \begin{bmatrix} j\left[E_\theta(\theta_p,\phi_q)\right] \\ \left[E_\phi(\theta_p,\phi_q)\right]\end{bmatrix}, \tag{6}$$

where the dagger † means pseudo-inverse, i.e. $\mathbf{P}^\dagger\mathbf{P} = \left[\left(\mathbf{P}^H\mathbf{P}\right)^{-1}\mathbf{P}^H\right]\mathbf{P} = \mathbf{I}$, and H is Hermitian. The total number of unknowns from both $[f_{mn}]$ and $[a_{mn}]$ is found as $2N(N+2)$. Thus, an initial number of sampled data would be $2N(N+2)$ with uniform sampling in θ and ϕ, though uniform sampling is not necessarily an optimal choice. If the $rank[\mathbf{P}]$ is $2N(N+2)$, the solution using the pseudo-inverse $\mathbf{P}^\dagger$ is exact under the assumption that the estimated N is correct. If $rank[\mathbf{P}]$ is smaller (under-determined system) or greater (over-determined system) than $2N(N+2)$, the solution becomes essentially a least-squares solution. For $rank[\mathbf{P}] < 2N(N+2)$, it suggests we have insufficient independent samples of near-field data or the estimated N is high. For a higher rank, the $rank[\mathbf{P}]$ can be reduced by eliminating singular values with a low amplitude due to numeric or measurement noise, as Wittmann [3] and Sarkar [8] demonstrated with singular value decomposition. If the rank of the reduced $\mathbf{P}$ indicates insufficient samples, we should consider increasing the number of sampled data (K) in the allowable scan angles. After the matrix inversion is accomplished, far-field patterns can be obtained using the far-field form of the scaled spherical coupling coefficients

$$f_{mn,FF} = r_0(j)^{n+1} f_{mn} / \hat{H}_n^{(2)} \text{ and } a_{mn,FF} = r_0(j)^n a_{mn} / \hat{H}_n^{(2)\prime}. \tag{7}$$

A flow chart of the direct matrix approach is shown in Figure 3.

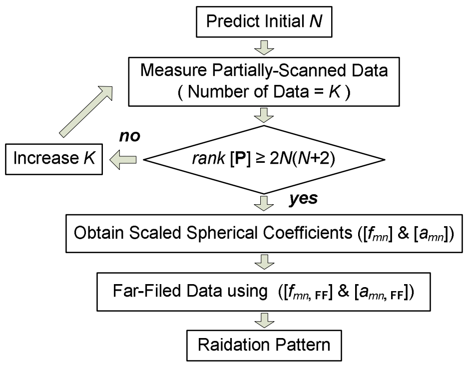

Figure 3. Flow chart of far-field radiation pattern estimation from a partially-scanned near-field data.

4. Examples Based on Simulated Partial Near-Field Data

In order to demonstrate the concept of the direct matrix approach, both omni-directional and directional antennas were considered, as shown in Figure 4. Uniformly-sampled, partial near-field data at 1.0 GHz for the mobile antenna ($r_0 = 0.75\ \lambda_0$) and 1.5 GHz for the horn antenna ($r_0 = 2.5\ \lambda_0$) was obtained from simulations with a commercial MoM code [9]. The flow-chart iteration was used to determine the highest-order spherical mode number (N), found as 6 and 10 for the mobile and horn antennas respectively. The final N is higher than the estimated N from Eqs. (4) and (5) because both equations are for far fields, but at least Eqs. (4) and (5) provide a starting point. The estimated 2-D far-field patterns using the direct matrix approach shown in Figure 5 provides good agreement with the simulated patterns. Since the estimated 3-D far-field patterns are very similar to the simulated 3-D patterns, only the estimated 3-D patterns are shown in Figure 5.

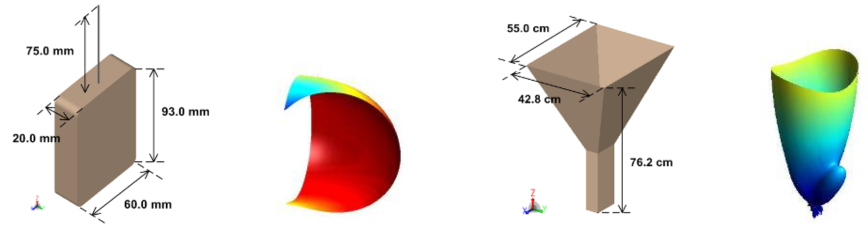

(a) (b) (c) (d)

Figure 4. Antenna geometry and partially-scanned near-field data for full 3-D far-field pattern reconstruction: (a) Geometry of a mobile antenna with 1-GHz resonance, (b) Partial near-field data of the mobile antenna, (c) Geometry of a horn antenna, and (d) Partial near-field data of the horn antenna (excluding the main beam).

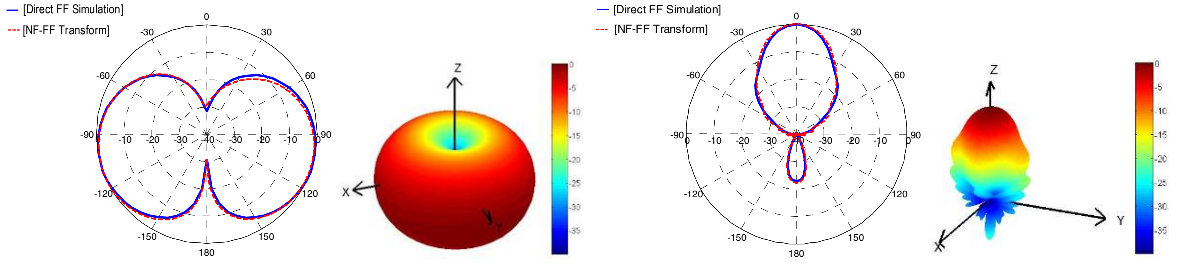

(a) (b) (c) (d)

Figure 5. Estimated 2-D and 3-D radiation patterns for the demonstrated examples: (a) Mobile antenna 2-D elevation cut on *xz*-plane, (b) Mobile antenna 3-D pattern, (c) Horn antenna 2-D elevation cut on *xz*-plane, and (d) Horn antenna 3-D pattern.

5. Conclusion

In this paper, we investigated radiation-pattern estimation from a subset of desired spherical near-field data. Antenna-field region and maximum-directivity estimation were discussed in terms of spherical-wave excitation to determine the highest-order spherical mode. A direct matrix approach was explained and examples provided to demonstrate the results. The examples were a mobile whip antenna and a horn antenna. The results show the direct matrix approach provides excellent agreement between the exact and estimated 3-D far-field patterns. An added benefit of this approach is the reduced scan time of the antenna measurement.

6. References

1. A. D. Yaghjian, “An Overview of Near-Field Antenna Measurement,” *IEEE Trans. Antennas Propag.*, vol. 34, January 1986, pp. 30 – 45.

2. O. M. Bucci, G. D’Elia, and M. D. Migliore, “A New Method for Avoiding the Truncation Error in Near-Field Antennas Measurements,” *IEEE Trans. Antennas Propag.*, vol. 54, October 2006, pp. 2940 – 2952.

3. R. C. Wittmann, Stubenrauch C. F., and C. F. Francis, “Spherical Scanning Measurements using Truncated Data Sets,” *Antenna Measurement Techniques Association Proceedings*, November 2002, pp. 279 – 283.

4. J. E. Hansen, *Spherical Near-Field Antenna Measurements*, Peter Peregrinus Ltd., London, 1988.

5. W. L. Stutzman and G. A. Thiele, *Antenna Theory and Design*, 2nd Ed., John Wiley & Sons, New York, 1998.

6. R. F. Harrington, “Effect of Antenna Size on Gain, Bandwidth, and Efficiency,” *Journal of Research of the National Bureau of Standards*, vol. 64D, January-February 1960, pp. 1 – 12.

7. J. R. Iames and L. W. Longdon, “Prediction of Arbitrary Electromagnetic Fields from Measured Data,” *Alta Frequenza*, vol. 38, May 1969, pp. 286 - 290.

8. T. K. Sarkar and A. Taaghol, “Near-fIeld to Near/Far-Field Transformation for Arbitrary Near-Field Geometry Utilizing an Equivalent Electric Current and MoM,” *IEEE Trans. Antennas Propag.*, vol. 47, March 1999, pp. 566 – 573.

9. EM Software and Systems, FEKO Suite version 5.5 (http://www/feko.info).